Dynamic light scattering in network-forming sodium ultraphosphate liquids near the glass transition

R. Fabian, Jr. and D. L. Sidebottom
Physics Department, Creighton University, 2500 California Plaza, Omaha, Nebraska 68178, USA
(Received 25 February 2009; revised manuscript received 9 May 2009; published 26 August 2009)

The viscoelastic relaxation of glass-forming $(Na_2O)_x(P_2O_5)_{1-x}$ liquids was measured by photon correlation spectroscopy at temperatures near the glass transition for compositions extending from pure phosphorus pentoxide to the metaphosphate ($x=0.5$). Over this compositional range, alkali addition produces a continuous depolymerization of the covalently bonded structure from one of a three-dimensional network to that of polymer chains. Substantial increases in the fragility accompany the depolymerization and are shown to be *identical* to those seen in certain ion-free chalcogenide glass formers suggesting the time scale for viscoelastic relaxation in network-forming liquids is controlled only by the topology of the covalent structure. The relaxation is nonexponential and the stretching exponent shows a complex variation with regards to both composition and temperature that is believed to arise from a decoupling of ionic motions from those of the network occurring as the glass transition is approached.

DOI: 10.1103/PhysRevB.80.064201 PACS number(s): 64.70.ph, 61.43.Fs, 66.20.Ej, 78.35.+c

I. INTRODUCTION

Although most liquids crystallize when cooled, it appears that all liquids have the potential to form a noncrystalline solid if cooled rapidly enough. For this reason, the glass transition remains an active area of research.[1–3] Over the years, numerous experimental studies and many theoretical descriptions have appeared that have done much to provide insight on the nature of this ergodic-to-nonergodic transition.[4–7] Central to many of these studies is the development of an understanding of the viscoelastic properties of the supercooled, disordered, liquid whose viscosity can, in many instances, increase tenfold for only a mere 5 K decrease in temperature near the transition. The viscoelastic relaxation of the liquid is simultaneously nonexponential and non-Arrhenius and readily characterized by the time-dependent dynamic structure factor (obtained for a specific scattering wave vector q). The dynamic structure factor displays a two-step decay[4] in which fast, localized motions (β relaxation or Johari-Goldstein secondary relaxation[8]) are separated from the collective, viscoelastic (VE) flow (α relaxation) by a plateau known as the nonergodic level. The slower VE relaxation is nonexponential and well approximated by a stretched exponential

$$S_q(t) = f_q \exp[-(t/\tau)^{\beta}], \tag{1}$$

where β is the stretching exponent, f_q the nonergodic level, and the average VE relaxation time is given as $\tau_{\text{avg}} = \frac{\Gamma(1/\beta)}{\beta}\tau$, where $\Gamma(z)$ is the gamma function. Above the transition, the liquid is ergodic and $S_q(t)$ decays to zero in the long-time limit. Below the transition, the α relaxation becomes arrested and ensemble-averaged measurements of $S_q(t)$ exhibit a nonzero constant (f_q) at long times. Although the term "nonergodic level" was introduced in mode coupling theory descriptions of the glass transition, here it is synonymous with the fraction of $S_q(t)$ that decays by viscoelastic flow.

The VE relaxation time generally follows a non-Arrhenius temperature dependence and is often described by a modified Arrhenius law

$$\tau_{\text{avg}} = \tau_o \exp[B/(T-T_o)]. \tag{2}$$

Although the VE relaxation is only truly arrested at T_o, it is conventional to assign the glass transition, T_g, to the temperature at which the VE relaxation time is on the order of 100 s.

A major advance in understanding the nature of the glass transition was the introduction over 20 years ago of the concept of fragility[9,10] which has since developed into a guiding paradigm for interpreting the relationships between dynamics of a supercooled liquid and its incipient glass structure. For fragile liquids, $T_o \leq T_g$ and the relaxation time increases most sharply just near T_g. These materials are populated by many simple molecular liquids held together by van der Waals forces that form nondirectional bonds. In these materials, the relatively weak and isotropic forces lend themselves to flow that is believed to involve a highly cooperative rearrangement of molecular units. At the opposite extreme are strong liquids which display a nearly Arrhenius behavior with $T_o \ll T_g$. These strong liquids are most typified by network-forming oxides that form a continuous network of covalent bonds with discrete coordination and in which flow is believed to stem from the random breaking and reformation of bonds for which cooperativity is largely absent. The rapidness with which the VE relaxation time increases near T_g is often characterized by the fragility index[11]

$$m = d \log_{10} \tau_{\text{avg}}/d(T_g/T)\big|_{T\to T_g}, \tag{3}$$

which has provided a convenient measure of the fragility for a diverse population of glass-forming liquids.

Since its introduction, many have explored potential correlations of structural, kinetic, and thermodynamic quantities to the fragility.[10,11] Angell[10] noted that the excess heat capacity of the liquid (relative to the glass) was generally larger for fragile liquids than for strong liquids. Bohmer *et al.*[11] analyzed a large volume of literature data to demonstrate that fragile liquids generally display a greater degree of nonexponentiality at T_g (i.e., smaller β) than strong liquids, sug-

gesting that nonexponentiality stems from a broadened distribution of relaxation rates bred by the greater level of cooperativity involved in viscous flow. In addition, Novikov and Sokolov[12] and Scopigno *et al.*,[13] respectively, highlighted correlations of the fragility to the Poisson ratio and the Debye-Waller factor seen in the solid phase. Lastly, we recently reported[14] a correlation of fragility to the nonergodic level found in the liquid phase as measured directly by dynamic light scattering.

While the establishment of such global correlations is insightful, in most all cases, there are materials that, for whatever reason, fail to conform. As an example, Angell[10] noted that alcohols violated the correlation of fragility with excess heat capacity. Similarly, the correlations observed by Novikov and Sokolov[12] and Scopigno *et al.*[13] appear to be unsuccessful when larger data sets are included.[15–17] In an effort to better understand the connections between structure and dynamics, we believe it is fruitful to investigate the connection *directly* by studying a single glass-forming system for which the structure is well-characterized and can be systematically altered to produce significant changes in fragility. Here, we report findings of a unique study of the liquid dynamics in glass-forming sodium ultraphosphate liquids near T_g obtained by photon correlation spectroscopy.

Amorphous P_2O_5 forms a three-dimensional covalent network with three bridging oxygens per phosphate unit (a fourth oxygen is double bonded) and the network can be depolymerized[18,19] in a systematic manner by addition of an alkali oxide (Na_2O). In this sense, the depolymerization is similar to that occurring in network-forming chalcogenide glasses composed of covalently bonded mixtures of Se, As, and Ge whose average bond coordination can be varied from upwards of $\langle r\rangle=2.7$ (three-dimensional networks) to $\langle r\rangle=2$ (polymer chains) merely by manipulation of the composition.[20–23] Studies of the chalcogenides have been driven in part by theoretical considerations[24,25] of random covalent networks that predict a special rigidity percolation to occur at $\langle r_c\rangle=2.4$ where the number of constraints balances the number of degrees of freedom. Since that prediction, several studies have observed anomalies in the chalcogenides near $\langle r_c\rangle$ including a minimum in the excess heat capacity[21] and a shallow minimum in the fragility.[22]

Interestingly, despite the presence of alkali ions which arise as a by-product of the depolymerization of the phosphate network, we observe changes of the fragility with respect to $\langle r\rangle$ in the ultraphosphate liquids that are *identical* to that observed for the ion-free chalcogenides, including a shallow minimum near the rigidity percolation threshold. This common evolution of the fragility in these network-forming systems is evidence that the fragility is predominantly controlled by the covalent network irrespective of the degree of ionic cross linking that may form. The presence of the alkali ions does, however, influence both the nonexponentiality and the nonergodic level.

II. EXPERIMENT

Samples of $(Na_2O)_x(P_2O_5)_{1-x}$ were obtained by two routes. P_2O_5 is notoriously hygroscopic and for compositions below 35 mol %, P_2O_5 (99.99%) was sublimed at 320 °C under vacuum and mixed with $NaPO_3$ in a glove box. The mixture was loaded into a precleaned silica ampoule and flame sealed under vacuum (approximately 60 mTorr). Samples were then melted at 900 °C for 2–4 h before conducting light-scattering studies. For compositions of 35 mol % and higher, moisture is less problematic[18] and samples were obtained by reacting Na_2CO_3 with $NH_4H_2PO_4$ and remelting in an open silica ampoule.

In some instances, notably at high phosphate content, a slight film formed on the interior wall of the ampoule during the melting procedure. This film was not visible by the naked eye, but became evident when the sample was placed in the focused beam of the laser. Although the film did diminish as procedures to eliminate water improved, it might also be the result of a reaction of silica with P_2O_5 gas occurring during the melting process. In a study of lanthanum phosphates, Park and Kreidler[26] reported mass changes during the melting of lanthanum pentaphosphate ($La_2O_3:5P_2O_5$) which were attributed to a reaction of P_2O_5 vapor with silica: silica acting as a sink for $P_2O_5(g)$. This reaction could potentially alter the composition of our sample. However, if we reason that the reaction ceases when a film of, say, 0.1 μm has formed, we estimate (based on the dimensions of our ampoule and the volume of sample) that the loss of P_2O_5 amounts to only 0.03 wt % and would have a negligible effect on our compositions. After melting, the lower section of the ampoule that comprises the liquid was gently torched to remove any residue forming on the interior wall. This was successful for all but pure P_2O_5 which became highly unstable when torched and prone to explode.

Photon correlation spectroscopy was performed at selected temperatures above T_g. Vertically polarized incident light (532 nm) was provided by a diode-pumped solid-state laser and focused into the ampoule interior. The vertically polarized component of the light scattered at a 90° scattering angle was imaged onto a pinhole (50 μm) and allowed to diffract through some distance onto the photocathode of a low-noise photomultiplier tube. The diffraction by the pinhole in relation to the area of the photocathode determines a signal-to-noise ratio for detecting intensity fluctuations known as the coherence factor,[27] A_{coh}. The coherence factor was calibrated separately by scattering from a aqueous suspension of polystyrene spheres (0.1 μm diameter) under identical optical conditions. After conditioning, the intensity signal from the photomultiplier tube was processed by a commercial correlator to produce the intensity autocorrelation function, $C(t)$, which is related to the dynamic structure factor as[28]

$$C(t) = 1 + A_{coh}|S_q(t)|^2.$$

Temperature control of the sample was obtained with a home-built optical furnace consisting of a stainless-steel cylinder, bored vertically to accommodate the ampoule, whose temperature was actively controlled to ±0.1 K by an electrical heating coil.

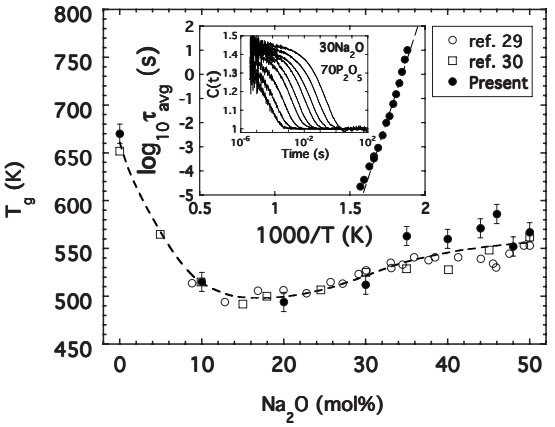

FIG. 1. Variation of the glass transition temperature with alkali oxide content. Inset shows the relaxation time plotted against inverse temperature for a liquid with $x=0.30$ demonstrating the determination of T_g. Inner inset shows typical autocorrelation spectra for the same composition at 602.4, 592.4, 582.1, 574.0, 567.0, 559.1, 553.1, 546.6, and 541.5 K.

III. RESULTS AND DISCUSSION

The inset to Fig. 1 shows a typical set of intensity autocorrelation functions obtained for a liquid containing 30 mol % Na_2O at several temperatures near T_g. Data such as these were collected for all compositions studied and were individually fit to Eq. (1) to obtain relevant parameters: f_q, β, and τ_{avg}. From $\tau_{avg}(T)$, an Arrhenius plot could then be constructed (see inset) and an extrapolation to $\tau_{avg}=100$ s was performed to determine the glass transition temperature of each composition. Values of T_g determined in this manner are shown in Fig. 1 together with data from the literature.[29,30] Reasonable agreement is found throughout the entire compositional range and is evidence for the integrity of the sample preparation techniques as regards the elimination of water.

The variation of T_g with alkali addition shows a rapid decrease to a minimum near 20 mol % Na_2O followed by a slight increase. This compositional dependence has been discussed by others[19,31] and is believed to result from the particular coordination demands of the alkali ion. Alkali addition depolymerizes the covalent network, but at compositions below about 20 mol %, the added alkali assumes isolated positions within the network, owing to an excess of terminal oxygens available to satisfy the coordination need of the ion. Above about 20 mol %, the ion's demand for coordination begins to exceed the available numbers of terminal oxygens. In this instance, the ions are forced to share terminal oxygens and begin to produce a level of *cross linking* between sections of the covalent network.[19] As a result, the cohesion lost by depolymerization is partially offset by the formation of active ionic cross links and the glass transition temperature increases.

Armed now with the T_g, we can plot the relaxation times in the form of a fragility plot.[10] This is done in Fig. 2 where data from all the compositions studied are included. For each, the fragility was determined from the slope of the line that passes through 100 s at $T_g/T=1$ and which best accommodates those data points lying within the practical limits

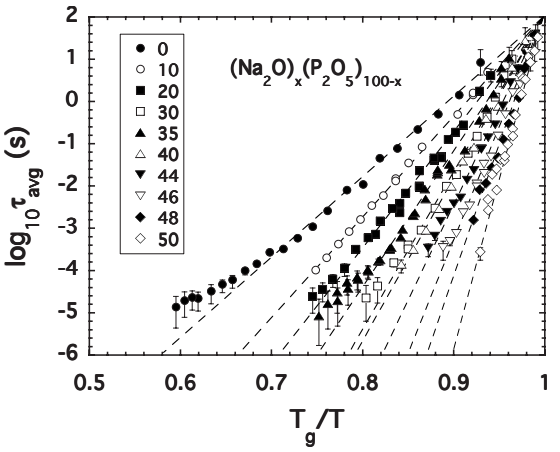

FIG. 2. Fragility plot of the average relaxation time vs inverse temperature scaled to T_g for all compositions (mol % listed in key) studied.

($\tau_{avg}\approx 100$ μs-10 s) of our photon correlation spectroscopy window. We observe a nearly systematic increase in the fragility with alkali addition that is not surprising given the systematic depolymerization of the covalent network that occurs. Nevertheless, to gain further insight, we have plotted the fragility index as a function of the bond coordination $\langle r\rangle$. This is shown in Fig. 3, together with data for the chalcogenide glasses reported by Bohmer.[21,22] For the ultraphosphates, the structure is well characterized and NMR studies[19] have documented how the conversion from phosphate units with three bridging oxygens to two bridging oxygens occurs in a systematic manner consistent with statistical considerations. This allows the bond coordination to be determined[19] for a given mol % Na_2O as $\langle r\rangle=2[x/(1-x)]+3[(1-2x)/(1-x)]$.

A remarkable coincidence between the evolution of fragility of both the chalcogenides and the ultraphosphates as a function of the bond coordination is evident. Both begin near $m=80$ for the structures composed of polymeric covalent chains ($\langle r\rangle=2$) and decrease to a shallow local minimum near $\langle r_c\rangle=2.4$ before increasing slightly. Data for the chalcogenides terminate at $\langle r\rangle=2.7$ due to limitations in its glass

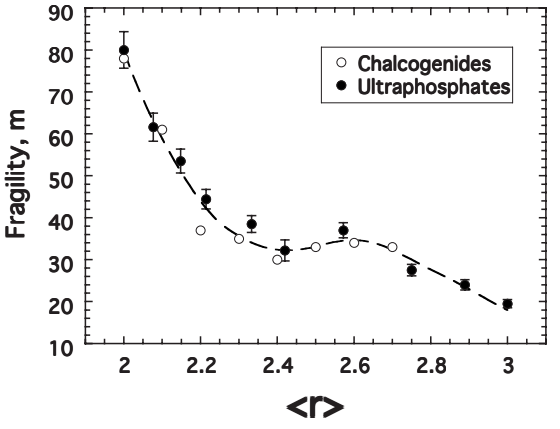

FIG. 3. Variation of the fragility index with bond coordination for both the ultraphosphate liquids and the chalcogenides (Refs. 21 and 22). Dashed line is only a guide.

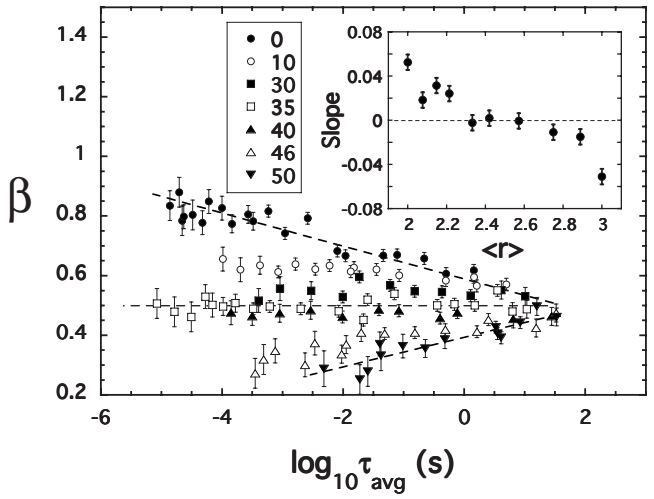

FIG. 4. Variation of the stretching exponent vs average relaxation time for ultraphosphate liquids. Dashed lines indicate the various temperature dependences discussed in the text. Inset shows how the slope $(d\beta/d\log_{10}\tau_{avg})$ varies with the bond coordination.

formation, but for ultraphosphates, the fragility then continues to decrease reaching a value of $m=20\pm1$ seen for pure P_2O_5. The near equivalence for these two systems indicates that, although the ultraphosphates possess a varying degree of ionic bonding, the fragility in these network-forming systems is dominated entirely by the bond density of the covalent network alone.

Next, we turn attention to the nonexponentiality of the relaxation as conveyed by the smallness of the stretching exponent, β, obtained in curve fitting Eq. (1). Figure 4 displays the values of β obtained as a function of the relaxation time. In Fig. 4, we see a complex evolution of the nonexponentiality both as T_g is approached and as alkali is added. For compositions up to about 30 mol %, β decreases as T_g (i.e., $\tau_{avg}=100$ s) is approached. Such temperature dependence is often reported in the literature[32] and is in fact similar to that seen in the mechanical relaxation[22] of the chalcogenides. However, for compositions greater than about 40 mol % Na_2O, the temperature dependence of β *reverses* and increases on approach to T_g. In the inset to Fig. 4, we have plotted the slope $(d\beta/d\log_{10}\tau_{avg})$ as a function of the bond coordination and note that the slope passes through zero (a situation of thermorheological simplicity) near the rigidity percolation threshold.

While there are some instances of β increasing as T_g is approached scattered in the literature, this is rarely observed[32] and requires some discussion. One clue to the diversity of slope found in Fig. 4 may be seen in how all the compositions tend toward a common value of $\beta\approx0.5$ as T_g is approached. Recall that the smallness of β is commonly associated with the degree of cooperativity in the relaxation and has been shown to generally decrease with increasing fragility.[11] Far from T_g, we see that increasing levels of alkali produce a lowering of the β and an increase in cooperativity consistent with the increasing fragility. This lowering of β indicates a broadening of the distribution of relaxation times present throughout regions of the material created by the increased mixing of Na with PO_4 units leading to greater diversity of local environments: alkali-rich regions dominated by ionic cross links and alkali-lean regions composed mainly of covalent structure. However, as T_g is approached, this correspondence between β and m disappears and the presence or absence of alkali ions becomes inconsequential to the observed value of β.

Far above T_g, added alkali promote increased cooperativity. But what is it that would serve to "turn off" this cooperativity as T_g is approached? The answer we believe lies in the concept of decoupling.[33,34] Many have noted that near T_g, the motion of mobile ions in a glass-forming liquid becomes decoupled from the viscoelastic relaxation.[33] Indeed, while the viscoelastic relaxation is arrested at T_g, ion motion continues to occur in the solid where ions migrate along the preferential pathways formed by charge-compensating sites (here the nonbridging oxygens) of the glass network.[35] However, as T increases in the liquid, the relaxation times of both the ion motion and the VE relaxation tend to converge.[33] Thus we believe the complex pattern shown in Fig. 4 is a consequence of this decoupling process. At high T, network and ions are coupled. Details of the VE relaxation are then sensitive to ion movements and the response becomes broadened relative to the broadening that would have been present for an ion-free network alone. However, as T approaches T_g, the ion motion becomes progressively decoupled and the VE relaxation becomes progressively insensitive to ion movements. The broadening then begins to mimic that of an ion-free network.

Finally, we consider our last fitting parameter, the nonergodic level. Accurate determination of this parameter is more difficult than the other two as it is not only dependent on calibration of the coherence factor but can also be compromised by stray, elastically scattered light whose intensity can lead to heterodyne[28] detection and an artificial lowering of the amplitude of the intensity autocorrelation. Recent improvements in sample preparation resulted in clearly defined scattering volumes free of stray light with the exception of P_2O_5 for which the $C(t)$ was obtained with a small quantity (intensity comparable to that from the scattering volume) of diffuse scattering from the ampoule wall. In Fig. 5, we plot the nonergodic level observed near T_g for our ultraphosphate samples along with values reported previously[14] for other glass-forming liquids including two network-forming oxides (B_2O_3 and As_2O_3) and several molecular liquids (orthoterphenyl, salol, and $0.4Ca(NO_3)_2$-$0.6KNO_3$ as well as values observed for a hard-sphere liquid in molecular-dynamics simulations. In the previous study,[14] we highlighted the interesting correlation between the nonergodic level and the inverse fragility (as depicted by the dashed line); a correlation that is congruent with a similar correlation[13,36,37] reported for the Debye-Waller factor of the solid phase. The implication of this correlation is that as fragility increases, a greater portion of the structure decays in the form of fast, localized relaxations with the partition between fast and slow decays approaching about 50% in the high fragility limit.

For ultraphosphates with less than about 35 mol % Na_2O, the nonergodic level conforms to our previous trend. However, at higher alkali contents, there is a noticeable deviation in which the nonergodic level exceeds the original correlation (dashed line) by roughly 15%. Apparently, the correla-

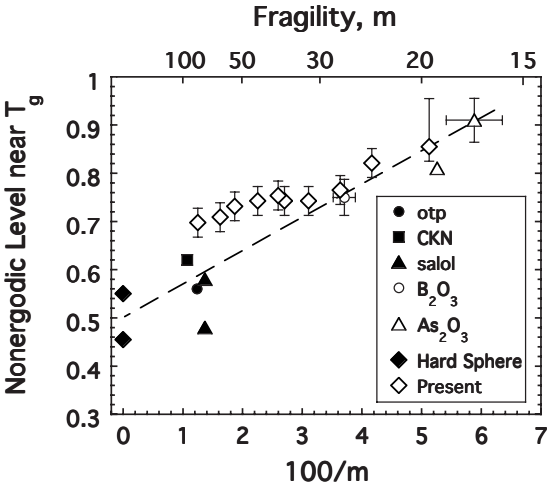

FIG. 5. Variation of the nonergodic level vs inverse fragility index for the ultraphosphate liquids (open diamonds) together with several glass-forming liquids (Ref. 14). Dashed line indicates a potential correlation discussed in the text.

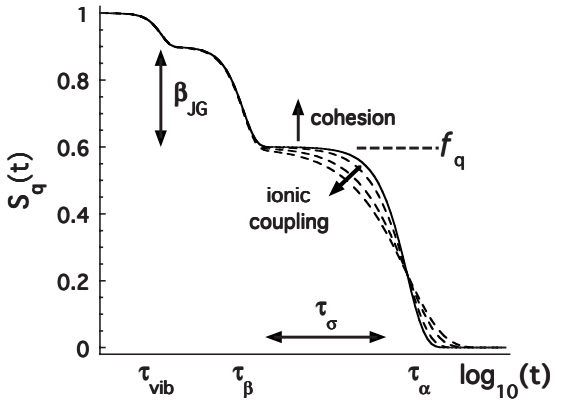

FIG. 6. A schematic representation of the dynamic structure factor. Aside from vibrational motions, fast localized motions produce a decrease to the nonergodic level. The level itself is set by the overall cohesion of the liquid. Depending on the level of ion coupling, the viscoelastic relaxation experiences earlier decay (dashed lines) in advance of the viscoelastic relaxation time.

tion is flawed, but what is the source for this deviation? We believe the answer lies in the changes in ion coordination discussed earlier with regards to the glass transition temperature. Recall that below 20 mol %, alkali enters the covalent network as isolated ions which are ineffective at cross linking the covalent network while at higher concentrations, the coordination demands of the cation exceed the available terminal oxygens and alkali becomes more effective in cross linking the depolymerized covalent network. In Fig. 5, we see that at compositions below 20 mol %, where alkali are ineffective in cross linking, the depolymerization results in a lowering of f_q in agreement with our previous trend. Recall also that the fragility index (the independent variable in Fig. 5) was insensitive to cross linking and found to only depend on the polymerization of the covalent network. We might reason then that had cross linking not developed alongside the depolymerization, f_q might have followed our previously observed trend. But cross linking does become effective above 20 mol % and we believe generates greater cohesion of the liquid producing not only an increase in the glass transition temperature but also a reduction of the faster localized relaxations and thus a lifting of the nonergodic level from the anticipated trend in Fig. 5. In the future, we hope to apply photon-correlation spectroscopy to chalcogenide liquids in an effort to resolve this issue.

IV. CONCLUSIONS

Let us conclude by drawing together all our findings to construct a physical picture behind the time evolution of the dynamic structure factor. We begin by examining the physical meaning of $S_q(t)$. The dynamic structure factor discussed here is the spatial Fourier transform of the van Hove correlation function, $G(r,t)$, which itself is the ensemble-averaged correlation of density fluctuations in space and time[28]

$$G(\vec{r},t) = \frac{\langle \delta\rho(0,0)\,\delta\rho(\vec{r},t)\rangle}{\langle \delta\rho\rangle^2}. \tag{4}$$

Physically, $G(r,t)$ is a measure of the likelihood that, given there is a density fluctuation at the origin at $t=0$, there will also exist a fluctuation some distance r away at a later time. Hence,

$$S_q(t) = \frac{\langle \delta\rho_q(0)\,\delta\rho_q(t)\rangle}{\langle \delta\rho_q\rangle^2}, \tag{5}$$

where

$$\delta\rho_q(t) = \int \delta\rho(\vec{r},t)e^{-i\vec{q}\cdot\vec{r}}d^3\vec{r}. \tag{6}$$

In any scattering experiment, the inverse of the scattering wave vector, q^{-1}, sets a relevant length scale over which the density fluctuations are monitored. For visible light. this length scale is roughly 10^3 Å and for P_2O_5 with a density of about 2.5 g/cm^3,[19] corresponds to a region of space containing on the order of 10^7 molecular units. Thus, we may view $S_q(t)$ as a measure of the temporal probability that two fluctuations of size $q^{-1} \approx 10^3$ Å separated by a distance of $q^{-1} \approx 10^3$ Å will remain correlated over time.

To assemble the features of $S_q(t)$, we imagine frames of a motion picture of the liquid played out over time. Our first frame captures the system in a particular initial configuration correlated with itself in the next instant and so $S_q(t)$ begins at unity. Vibrational motions are present everywhere occurring on a time scale τ_{vib}. The positions of the atomic centers make small excursions about their equilibrium positions and produce a small erosion of the initial correlation resulting in a small decrease in $S_q(t)$ as shown schematically in Fig. 6.

At longer times, the equilibrium positions of the vibrating atoms begin to execute small excursions which are attributed either to the anharmonicity of the elastic potential[37] or, in the case of a van der Waals liquid, a cage effect[4] wherein atoms make excursions within a cage formed by the nearest-neighbor coordination shell. In any event, this fast, localized motion (Johari-Goldstein secondary relaxation) again results in a further loss of correlation with a decrease in $S_q(t)$ occurring at some time scale τ_β and represents the first step in the two-step decay discussed in Sec. I. At this point, the level of

$S_q(t)$ is f_q, the nonergodic level, which is frozen in below T_g but which above T_g eventually decays on the VE time scale, $\tau_{avg}(\equiv\tau_\alpha)$.

In our discussion regarding Fig. 5, we have argued that the nonergodic level represents a measure of the overall cohesion present in the liquid (originating both from covalent bonds and active ion cross links). One sees that the strongest glass-forming liquids (the limit of m is 16) exhibit values of f_q approaching 0.95. As bonds are progressively removed from the covalent network, rigidity is reduced and the fast localized motions are amplified resulting in a decrease of the nonergodic level. Indeed, below the rigidity threshold, the once-percolated network vanishes and floppy modes[24] begin to appear. When ions are present, the cohesion lost by depolymerization is partially restored by ionic cross linking.

Between τ_β and τ_α resides the ion motions associated with ion conduction. In ion-conducting glasses, ions spend most of their time near a charge-compensating site (here the nonbridging oxygen) "wiggling" about.[38] Every once in a while, they hop to another site (on a time scale τ_σ) a short ($\approx$5 Å) distance away and are replaced by yet another ion. This hopping process itself occurs very rapidly and τ_σ is really a measure of the waiting time between hops.

But what effect does this short-range ion hopping produce with regards to $S_q(t)$? We argue that there would be no separate relaxation seen in $S_q(t)$ associated with the roughly 5 Å scale ion hopping in our situation where $q^{-1}\approx 10^3$ Å. This is particularly true in the situation of highly decoupled motion in which the charge-compensating sites (affixed to the network) may undergo the fast localized (Johari-Goldstein) motions on time scales of τ_β, but are otherwise stable on time scales of order τ_σ. Ion hopping merely *replaces* one wiggling ion at a given fixed site by another identically wiggling ion. Viewed on a 10^3 Å length scale, the level of correlation is no more eroded after the hop than before and hence there is no decay in $S_q(t)$ associated with ionic hopping.

However, when ion motion becomes coupled with the VE relaxation, ion hopping begins to lose its discrete character. Ions and network begin to rearrange in a concerted fashion. Cooperatively is enhanced and the result is the appearance of a more nonexponential VE decay with a corresponding decrease in the stretching exponent.

V. SUMMARY

The VE relaxation in network-forming ultraphosphate liquids displays a rich variation with alkali composition. The fragility of these liquids mimics that of ion-free chalcogenide liquids suggesting that fragility is controlled entirely by the covalent structure regardless of ionic cross linking. Despite this, the shape of the relaxation is sensitive to ion content provided ion motions are sufficiently coupled. The amplitude of the α relaxation appears to be determined by the overall cohesion of the network and decreases with increasing depolymerization.

ACKNOWLEDGMENT

Acknowledgment is made to the donors of The American Chemical Society Petroleum Research Fund (Grant No. 43743-GB10) for support of this research.

[1] M. D. Ediger, C. A. Angell, and S. R. Nagel, J. Phys. Chem. **100**, 13200 (1996).
[2] P. G. Debenedetti and F. H. Stillinger, Nature (London) **410**, 259 (2001).
[3] K. L. Ngai, J. Non-Cryst. Solids **275**, 7 (2000).
[4] W. Goetze, in *Liquids, Freezing, and the Glass Transition*, edited by J. P. Hansen, D. Levesque, and J. Zinn-Justin (North Holland, Amsterdam, 1990).
[5] M. H. Cohen and G. S. Grest, Phys. Rev. B **20**, 1077 (1979).
[6] G. Adam and J. H. Gibbs, J. Chem. Phys. **43**, 139 (1965).
[7] V. Lubchenko and P. G. Wolynes, Annu. Rev. Phys. Chem. **58**, 235 (2007).
[8] G. P. Johari and M. Goldstein, J. Chem. Phys. **53**, 2372 (1970).
[9] W. T. Laughlin and D. R. Uhlmann, J. Phys. Chem. **76**, 2317 (1972).
[10] C. A. Angell, in *Relaxations in Complex Systems 1*, edited by K. Ngai and G. B. Wright (Natl. Technol. Inform. Ser., U.S. Dept. of Commerce, Springfield, VA, 1985).
[11] R. Bohmer, K. L. Ngai, C. A. Angell, and D. J. Plazek, J. Chem. Phys. **99**, 4201 (1993).
[12] V. N. Novikov and A. P. Sokolov, Nature (London) **431**, 961 (2004).
[13] T. Scopigno, G. Ruocco, F. Sette, and G. Monaco, Science **302**, 849 (2003).
[14] D. L. Sidebottom, B. V. Rodenburg, and J. R. Changstrom, Phys. Rev. B **75**, 132201 (2007).
[15] S. N. Yannopoulos and G. P. Johari, Nature (London) **442**, E7 (2006).
[16] D. H. Torchinsky, J. A. Johnson, and K. A. Nelson, J. Chem. Phys. **130**, 064502 (2009).
[17] K. Niss, C. Dalle-Ferrier, V. M. Giordano, G. Monaco, B. Frick, and C. Alba-Simionesco, J. Chem. Phys. **129**, 194513 (2008).
[18] S. W. Martin, Eur. J. Solid State Inorg. Chem. **28**, 163 (1991).
[19] R. K. Brow, J. Non-Cryst. Solids **263&264**, 1 (2000).
[20] B. L. Halfpap and S. M. Lindsay, Phys. Rev. Lett. **57**, 847 (1986).
[21] M. Tatsumisago, B. L. Halfpap, J. L. Green, S. M. Lindsay, and C. A. Angell, Phys. Rev. Lett. **64**, 1549 (1990).
[22] R. Bohmer and C. A. Angell, Phys. Rev. B **45**, 10091 (1992).
[23] U. Senapati and A. K. Varshneya, J. Non-Cryst. Solids **197**, 210 (1996).
[24] H. He and M. F. Thorpe, Phys. Rev. Lett. **54**, 2107 (1985).
[25] J. C. Phillips, J. Non-Cryst. Solids **34**, 153 (1979).
[26] H. D. Park and E. R. Kreidler, J. Am. Ceram. Soc. **67**, 23 (1984).
[27] N. C. Ford, Jr., in *Dynamic Light Scattering*, edited by R. Pecora (Plenum Press, New York, 1985), p. 7.
[28] B. J. Berne and R. Pecora, *Dynamic Light Scattering* (Wiley, New York, 1976).
[29] A. Eisenberg, H. Farb, and L. G. Cool, J. Polym. Sci., Part A-2

4, 855 (1966).
[30] J. J. Hudgens, R. K. Brow, D. R. Tallant, and S. W. Martin, J. Non-Cryst. Solids **223**, 21 (1998).
[31] U. Hoppe, G. Walter, R. Kranold, and D. Stachel, J. Non-Cryst. Solids **263&264**, 29 (2000).
[32] K. L. Ngai, R. W. Rendell, and D. J. Plazek, J. Chem. Phys. **94**, 3018 (1991).
[33] F. S. Howell, R. A. Bose, P. B. Macedo, and C. T. Moynihan, J. Phys. Chem. **78**, 639 (1974).
[34] C. A. Angell, Chem. Rev. **90**, 523 (1990).
[35] G. N. Greaves, J. Non-Cryst. Solids **71**, 203 (1985).
[36] K. L. Ngai, Philos. Mag. **84**, 1341 (2004).
[37] P. Bordat, F. Affouard, M. Descamps, and K. L. Ngai, Phys. Rev. Lett. **93**, 105502 (2004).
[38] K. Funke, Prog. Solid State Chem. **22**, 111 (1993).